GSC Advanced Research and Reviews

eISSN: 2582-4597 CODEN (USA): GARRC2

Cross Ref DOI: 10.30574/gscarr

Journal homepage: https://gsconlinepress.com/journals/gscarr/

(RESEARCH ARTICLE)

Check for updates

Biodegradation of zinc oxide nanoparticles by *Rhizopus stoloniferas*

Marwa Hussein Ali Talaa and Ihsan Flayyih Hasan AL-Jawhari *

College of Education for Pure Sciences- University of Thiqar – Iraq.

GSC Advanced Research and Reviews, 2025, 24(03), 153-169

Publication history: Received on 02 August 2025; revised on 10 September 2025; accepted on 12 September 2025

Article DOI: https://doi.org/10.30574/gscarr.2025.24.3.0276

Abstract

This study investigated the ability of Rhizopus stolinifer to degrade zinc oxide nanoparticles (ZnO-NPs). The fungal isolated from agricultural soil cultivated with wheat crop (Triticum aestivum L.) in Abada village, Al-Nasiriyah, southern Iraq, using the dilution method. Soil samples were collected at a depth of (5–15) cm, and the study was conducted for a period of four months. The results showed the ability of Rhizopus stolinifer to grow in solid media (Potato Dextrose Agar) supplemented with Zinc oxide nanoparticles, at different concentrations (100, 200, 300 mg) and in the presence of different carbon and nitrogen sources (Glucose, maltose) ($NaNO_3$, NH_4Cl) at different incubation temperatures (15, 25, 35 °C) in the liquid mineral medium. The results showed a decrease in the pH value in varying ways: pH = (3.0 ,3.0,3.0) at a temperature of 15 °C, pH = (3.0, 3.0, 4.0) at a temperature of 25 °C, and pH = (3.0, 3.0, 3.0) and (3.0, 3.0, 4.0) in (Maltose + $NaNO_3$) at a temperature of 35 °C after 7 days incubation. The result confirmed the ability of Rhizopus stolonifer to biodegrade ZnO-NPs.

Keywords: Biodegradation; Fungi; Liquid Medium; Nanoparticles; Soil

1. Introduction

Nanotechnology has introduced novel engineered materials into environmental and agricultural systems, among which zinc oxide nanoparticles (ZnO NPs) have drawn increasing attention due to their multifunctional applications and widespread release into soils. Once deposited in terrestrial environments, ZnO NPs undergo interactions with soil chemistry and physical structures that critically affect their mobility, dissolution, and ecological fate. Several studies have highlighted that Zn contamination of soils originates from industrial emissions, excessive use of fertilizers, mining, and sewage discharges, leading to disruptions in soil chemical and biological properties and a subsequent decline in fertility and productivity [1].

The presence of ZnO NPs in soils does not only threatens soil microorganisms but also poses significant risks to human health through entry into the food chain. When absorbed by crops, these nanoparticles can accumulate in edible plant tissues and eventually transfer to animals and humans, where they cause oxidative stress, inflammation, genotoxicity, and disturbances in major physiological systems. Reviews have emphasized that nanoparticles can cross biological barriers, inducing respiratory inflammation, neurotoxicity, immune dysfunction, reproductive impairments, and endocrine disruption, in addition to their potential carcinogenicity [2]. Such findings raise serious concerns about food safety and human exposure to nano-contaminants through dietary pathways.

At the same time, zinc oxide nanoparticles exhibit distinctive physicochemical properties, including high chemical stability, UV absorption capacity, and strong antimicrobial activity, which have supported their use in food, agricultural, and industrial applications. Different synthesis methods—chemical, physical, and biological—yield particles with variable size, shape, and surface charge, each influencing their reactivity and toxicological profile. While their small size and surface reactivity make them valuable as antimicrobial agents and nanofertilizers, these same features also drive

* Corresponding author: Ihsan Flayyih Hasan AL-Jawhari

their potential hazards by enhancing ion release, generation of reactive oxygen species (ROS), and disruption of cellular metabolism [3].

Soil fungi, which play key roles in nutrient cycling and organic matter decomposition, are particularly relevant in the biotransformation of ZnO NPs. This process not only detoxifies the nanoparticles but also highlights the active contribution of fungi in geochemical cycling [4]. where the fungus has been utilized in mycosynthesis of ZnO NPs, producing biogenic particles with antimicrobial, anticancer, and antioxidant potential [5], further emphasizing the dual role of fungi as both sensitive bioindicators of nanoparticle stress and valuable agents for nanoparticle transformation.

Despite the global expansion of research on ZnO NPs, there remains a critical knowledge gap in Iraq. To date, no comprehensive study has examined the combined effects of ZnO nanoparticles on soils, fungi, and agricultural plants within Iraqi ecosystems. Therefore, the present study seeks to address this gap by investigating the interactions of ZnO NPs with local soils, their influence on fungal communities, and their impacts on plant growth. This effort not only contributes to understanding the environmental behavior and risks of ZnO NPs but also provides a foundation for future strategies to manage nanoparticle contamination in Iraq's agricultural systems.

2. Materials and Methods

2.1. Collection of Soil Samples

Soil samples were collected from agricultural land located in Abada village, Al-Fuhud district, Al-Nasiriyah (southern Iraq), an area cultivated with wheat (*Triticum aestivum L.*). The sampling process was carried out by removing the surface layer of soil at a depth of 5–15 cm, using clean and sterilized tools to prevent any external contamination. A composite sample of approximately 1 kg was obtained and immediately transferred into clean, sterile polyethylene bags for safe transportation to the laboratory. Upon arrival, the soil was thoroughly homogenized and then distributed into four Plant container pots, representing three treatment groups with different concentrations of zinc oxide nanoparticles (100, 200, and 300 mg per pot) in addition to one control Plant container without ZnO NPs. The experimental setup was maintained for about four months (16 weeks) under controlled conditions, with daily irrigation using distilled water.

2.1.1. Chemicals

- All chemicals used in the current study were sourced from BDH and Merch.
- Zinc oxide nano powder (Zano-NPs) was obtained from US Research Nanomaterials with a purity of 99%+ and an average particle size of 50 nm.

2.1.2. Media

- Potato Agar Dextrose (PDA): It consists of 200 gm of potatoes, 20 gm of dextrose and 20 gm of agar dissolved in a liter of distilled water Then it is sterilized in an autoclave at 120°C for 20 minutes and pressure 15 pounds.
- Mineral salt medium: It is used for the growth of fungi (Sharling and Gott, 1966) and consists of (K2HPO4, 1.71g; KH2PO4, 1.32g; NaNo3, 0.42g; MgSo4. 7H2O, 0.42g; CaCl2, 0.02g) the contents are dissolved in a liter of distilled water Then it is sterilized in an autoclave at 120°C for 20 minutes and pressure 15 pounds.

2.1.3. Isolation of fungi

The fungus was isolated from the agricultural soil collected from Abada village, Al-Fuhud district, Al-Nasiriyah (southern Iraq), which was cultivated with wheat (Triticum aestivum L.), using the dilution method and their specific culture media. The soil samples were transferred to the laboratory for the purpose of isolating and diagnosing the fungi present in them. The culture medium Potato Dextrose Agar (PDA) was used for fungal growth according to the method stated [6]. After homogenization, serial dilutions of 10^{-1}, 10^{-2}, and 10^{-4} were prepared. The pour-plate technique was applied by transferring 1 ml from the final dilution into sterile Petri dishes, followed by the addition of the PDA medium supplemented with 250 mg/L of the antibacterial agent Chloramphenicol to inhibit and prevent bacterial growth. The plates were gently rotated in a circular motion to ensure homogeneity, then incubated at 25 °C for 7 days. The numbers of fungi in the soil samples were estimated using the total counting method described by [6] with the PDA medium, and the results were expressed as the average number of fungal colonies per gram of soil sample.

2.2. Methods

2.2.1. Molecular Identification of Fungi that Degrade Zinc Oxide Nanoparticles

That internal transcribed spacer (ITS) region was amplified and sequenced in order to perform molecular identification. Using primers (ITS1 and ITS4), the internal transcription spacer region (ITS1–5.8S–ITS2) was amplified using polymerase chain reaction (PCR) technology. The source of these primers is Macrogen, Korea. Using the genomic DNA as a template and the ITS primers ITS1 (5π-GTGTTACCGGAGTAGGCCTC-3_R) and ITS4 (5π- ATGATCCTTCCGCAGGTCAC -3 $_R$), the ITS region was amplified using polymerase chain reaction (PCR). One microliter of isolated fungal genomic DNA, 0.5 micrograms of each primer, and 50 microliters of Maxima Hot Start PCR Master Mix (Thermo) made up the PCR mixture. Al-Ameen Foundation for Study and Research (Najaf, Iraq) used a DNA Engine Thermal Cycler to do the PCR with a hot start that lasted for four minutes at 94 °C, thirty cycles of 94 °C, 56 °C, and 72 °C, and a final extension that lasted for seven minutes at 72 °C. At Macrogen Company (Korea), a DNA sequencer was used for commercial sequencing. The NCBI BLAST tool was used to match the ITS sequence against the GenBank database. Then, using BLASTN, sequences were matched with ITS sequences in the GenBank database.

2.3. Biodegradation of Zinc Oxide Nanoparticles in Solid Mineral Media

The medium was prepared potato dextrose agar (PDA) in four 250 ml conical flasks and then sterilized with an autoclave device at a temperature of 121 °C and a pressure of 15 pounds/square inch for 20 minutes. After lowering the temperature of the medium to an appropriate level, zinc oxide nanoparticles (ZnO-NPs) were added at four concentrations: (0, 100, 200, 300) mg/L. The medium was then poured into sterilized Petri dishes with a diameter of 8.5 cm and left to dry for 30 minutes. Each dish was inoculated with the fungal inoculum by transferring a disc (4 mm in diameter) from a pure culture aged 7 days of *Rhizopus stolonifer* using a sterile corn borer to the center of the plate. The plates were then incubated at 25 °C for 7 days, and this experiment was carried out with three replications for each treatment. The growth rate of the fungus was calculated by measuring the diameter of the colony.

2.4. Biodegradation of Zinc Oxide Nanoparticles in Liquid Mineral Media

Mineral salt medium for fungal growth was prepared in twelve conical flasks with a capacity of 250 ml. The medium was sterilized in an autoclave at 121 °C and 15 psi for 20 minutes. Zinc oxide nanoparticles (ZnO-NPs) were added to the culture medium after cooling to an appropriate temperature at three concentrations (100, 200, and 300 mg/L), with three replicates for each concentration in addition to control flasks without ZnO-NPs. All flasks, except the control, were inoculated with the fungus *Rhizopus stolonifer* by transferring a 5 mm diameter disk from 7-day-old fungal cultures using a sterile corn borer. The cultures were incubated in a shaker incubator at 150 rpm at three temperatures (15 °C, 25 °C, and 35 °C) for 7 days. After incubation, the cultures were processed to separate the fungal mycelium by centrifugation. Specifically, 10 mg of sample was centrifuged at 100,000 rpm for 30 minutes, and the resulting supernatant was collected. The obtained solution was stored in dark containers in a refrigerator at 4 °C until FTIR analysis was performed to identify the changes associated with the biodegradation of ZnO nanoparticles.

2.5. Analysis using Fourier Transform Infrared spectroscopy

This analysis was conducted in the same way as the previous one, where the samples were analyzed using an FTIR device in the Directorate of Research and Renewable Energies, Ministry of Higher Education, Baghdad.

2.6. Statistical Analysis

All applications were analyzed using ANOVA in SPSS (version 25.0). All statistical tests were conducted at a significant level of $p > 0.05$.

3. Results and Discussion

3.1. Isolation of fungi

Filamentous fungi were isolated from agricultural soils in Abada village, Al-Fuhud district, Al-Nasiriyah, southern Iraq, using the dilution method. The results of Table No. 1 showed that Rhizopus stolinifer recorded the highest frequency of occurrence. The widespread presence of this fungus is attributed to its possession of an effective enzymatic system, including amylas, protease, and pectin-degrading enzymes, which enable it to utilize complex organic sources, as well as its ability to tolerate unfavorable environmental conditions and to spread easily through the abundant production of reproductive sporangiospores [7][8]. These fungi have also been reported by [9], who confirmed the significant role of Rhizopus stolonifer both as a saprophytic decomposer in soil ecosystems.

Table 1 Frequency of Species Isolated from the Surface of Soil

Fungi Species	The number of samples in which the fungal species appeared	Frequency%
Rhizopus stolonifer	16	100%

3.2. Molecular Diagnosis of Fungi

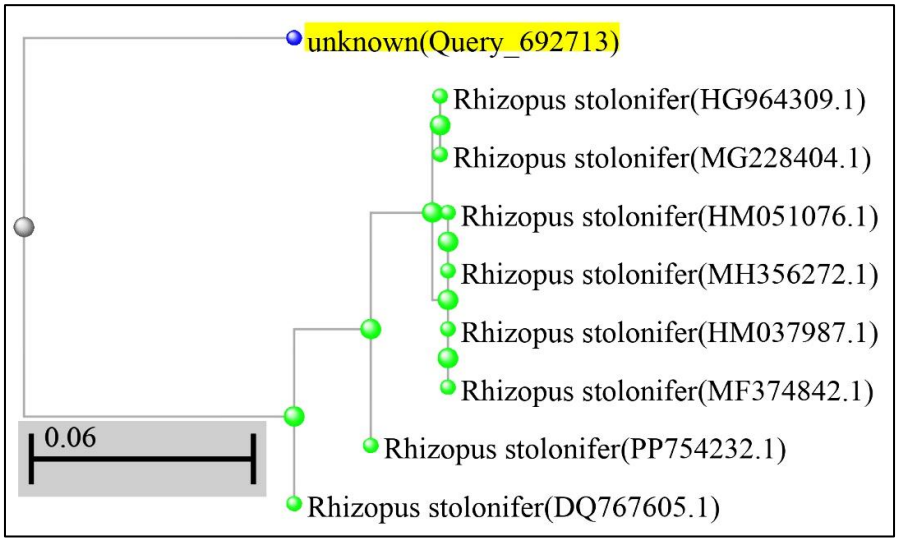

Figure 1 Phylogenetic Tree of ITS Sequences of the Fungal Isolate with the Sequences from NCBI and Designated as Rhizopus stolonifer

During this study, a number of fungi taken from agricultural soils in Abada village, Al-Fuhud district, Al-Nasiriyah, southern Iraq were isolated, and one fungal species was the most prominent in the samples. The taxonomic status of the fungal isolate was defined by sequencing ITS genes. The morphological culture characteristics as well as molecular identification based on ITS sequencing analysis for the isolate were consistent with Rhizopus stolonifer, as shown in Fig (1).

3.3. Biodegradation of Zinc Oxide Nanoparticles in Solid Medium

The growth of Rhizopus stolinifer on Potato Dextrose Agar (PDA) medium in the presence of different concentrations of zinc oxide nanoparticles (ZnO-NPs) is shown in Table (2). The colony diameter in the control treatment (0 mg/L) reached 8.00 cm after 7 days of incubation. When exposed to 100 mg/L ZnO-NPs, the colony diameter slightly decreased to 7.67 cm, and a further reduction was observed at 200 mg/L, where the colony diameter was 7.23 cm. At the highest concentration of 300 mg/L, the colony diameter reached 7.50 cm. These results indicate that R. stolinifer was able to maintain relatively stable growth on solid medium across all concentrations, with only slight differences compared to the control. This stability suggests that the fungus possesses a moderate resistance to ZnO-NPs and can adapt to their presence in the growth environment without significant inhibition of colony expansion. Similar findings were reported by [10], who described R. stolinifer as a fast-growing fungus with strong persistence, often requiring advanced control strategies, including nanomaterials like ZnO, to limit its spread in postharvest conditions. This agreement supports the current observation that the fungus maintains growth stability even under ZnO-NP exposure.

Table 2 Colony diameters of Rhizopus stolinifer grown on solid medium with ZnO-NPs

Fungi	Concentration				Mean
	Control	100 mg/L	200 mg/L	300 mg/L	
Rhizopus stolonifer	8.00 ± 0.00	7.67 ± 1.23	7.23 ± 0.87	7.50 ± 0.30	7.60 ± 0.72
L.S. D	0.005				

3.4. Biodegradation of Zinc Oxide Nanoparticles in Liquid Mineral Medium

The results of the current study showed the ability that Rhizopus stolinifer isolated from agricultural soils to biodegrade zinc oxide nanoparticles (ZnO-NPs) at concentrations of (100, 200, 300) mg in the liquid mineral medium treated with different carbon and nitrogen sources and at different temperatures (15, 25, 35) ℃.

The results shown in Tables (3 and 4) confirm that ZnO-NPs affected the dry weight of Rhizopus stolinifer biomass in liquid media. In maltose with $NaNO_3$ medium (Table 3), the dry weight increased from 0.10 gm in the control to 0.27 gm at 100 gm and reached 0.50 gm at 200 mg/L, before decreasing slightly to 0.39 mg at 300 mg/L. This pattern indicates that the fungus showed enhanced biomass production at low and moderate concentrations of ZnO-NPs, while growth was somewhat reduced at the highest concentration. These observations are in line with the findings of [11], who demonstrated that R. stolinifer utilized glucose more efficiently than maltose as a carbon source, which explains the relatively weaker performance in maltose-based media.

In glucose with NH_4Cl medium (Table 4), R. stolinifer also exhibited a clear response. The dry weight increased from 0.14 gm in control to 0.26 gm at 100 mg/L and 0.47 gm at 200 mg/L, with the highest value recorded at 0.67 gm under 300 mg/L. These results suggest that the type of medium influenced the fungal response, with glucose with NH_4Cl supporting greater biomass accumulation than maltose with $NaNO_3$ in the presence of ZnO-NPs. This trend agrees with [12], who reported that ammonium salts supported superior growth of R. stolinifer compared to nitrate sources, highlighting the fungus's preference for ammonium nitrogen in liquid media.

The variation in pH values (Table 5) further demonstrates the metabolic activity of R. stolinifer. In glucose with NH_4Cl medium, the initial pH of 8.0 decreased sharply to 3.0 at concentrations of 100–300 mg/L, while in maltose with $NaNO_3$ medium, the pH showed a similar reduction to 3.0 under ZnO-NP exposure. In both media, slight increases to 4.0 were observed under certain conditions, reflecting acid production and potential buffering effects. These findings confirm that R. stolinifer actively modified its environment by acidifying the medium, which may have facilitated interactions with and transformation of ZnO-NPs. This observation is consistent with [13], who found that R. stolinifer could grow in a wide pH range (3–10) but reduced the medium pH significantly through the secretion of organic acids. Moreover, the production of such acids aligns with the findings of [14], who demonstrated that the fungus metabolized sugars with ammonium nitrogen to yield primary metabolites such as fumaric and lactic acids, leading to substantial acidification of the growth medium.

The results of the analysis using Fourier-transform infrared spectroscopy (FTIR), as shown in Figures (3), (4), (5), (6), (7), and (8), demonstrated the ability of the fungus R. stolinifer to biodegrade ZnO-NPs at concentrations of 100, 200, and 300 mg in the mineral salt medium supplemented with different carbon and nitrogen sources (glucose + NH_4Cl, maltose + $NaNO_3$). Clear changes in the spectral bands were observed, including the appearance and disappearance of peaks in the regions (1500–2000), (500–1500), and (3000–3500), which indicated the formation of ester, carboxylic acid, and hydroxyl groups. These modifications confirm the active role of fungal metabolites in the transformation of nanoparticles. This result was similar to the findings of [15], who reported that biologically synthesized ZnO-NPs display characteristic FTIR signals reflecting microbial interaction, and in agreement with [16], who observed distinct FTIR shifts during the biodegradation of kerosene by R. stolinifer. Figure (2) represents the control ZnO-NPs at 25℃ and concentrations (100, 200, 300) mg.

Figures (9), (10), (11), (12), (13), and (14) showed the ability of R. stolinifer to biodegrade ZnO-NPs at concentrations of 100, 200, and 300 mg under different nutritional conditions (maltose + $NaNO_3$ and glucose + NH_4Cl). The FTIR spectra revealed the disappearance of several peaks in the mid-frequency region (500–1500) and the emergence of broad hydroxyl bands in the region (3000–3500), which indicated the presence of OH groups. These changes provide evidence of acid formation, likely resulting from the fermentation of glucose and the metabolic activities of the fungus. The results are consistent with [17], who demonstrated distinct FTIR band patterns produced by fungal metabolites during nanoparticle stabilization and transformation, and with [18], who observed ester and hydroxyl bands as evidence of fungal degradation of hydrocarbons.

Figures (15), (16), (17), (18), (19), and (20) illustrated the biodegradation of ZnO-NPs by R. stolinifer at concentrations of 100, 200, and 300 mg in mineral salt medium supplemented with either maltose + $NaNO_3$ or glucose + NH_4Cl. The FTIR spectra showed marked biotransformation, with shifts and disappearance of peaks in the regions (1000–1500) and (1500–2000), as well as the emergence of strong hydroxyl bands at (3000–3500). These spectral changes are direct evidence of the fungal degradation process and confirm the interaction of metabolites with ZnO nanoparticles. This finding is consistent with [19], who emphasized that environmental factors such as temperature strongly influence the fungal-mediated transformation of ZnO-NPs, as reflected in FTIR changes.

Table 3 Dry weight of R. stolinifer grown in maltose supplemented with $NaNO_3$ medium

Fungi	**Concentration**				**Mean**
	Control	100 mg/L	200 mg/L	300 mg/L	
Rhizopus stolinifer	0.10 ± 0.00	0.27 ± 0.02	0.50 ± 0.03	0.39 ± 0.49	0.32 ± 0.20
L.S.D	0.165				

Table 4 Dry weight of R. stolinifer grown in glucose supplemented with NH_4Cl medium

Fungi	**Concentration**				**Mean**
	Control	100 mg/L	200 mg/L	300 mg/L	
Rhizopus stilonifer	0.14 ± 0.00	0.26 ± 0.01	0.47 ± 0.02	0.67 ± 0.49	0.38 ± 0.13
L.S. D	0.000				

Table 5 Variation in pH Values in the Medium Treated with Zinc Oxide Nanoparticles Under Study by R. stolinifer

Fungus	**Medium**	**Concentration**				**Mean ± SD**
		Control	100 mg/L	200 mg/L	300 mg/L	
Rhizopus stolinifer	Glucose + NH_4Cl	8 ± 0.00	3 ± 0.58	3 ± 1.15	3 ± 0.58	4 ± 2.06
	Maltose + $NaNO_3$	8 ± 0.00	3 ± 1.00	3 ± 1.00	3 ± 1.00	4 ± 2.06
L.S. D	Glucose + NH_4Cl = 0.017					
	Maltose + $NaNO_3$ = 0.021					

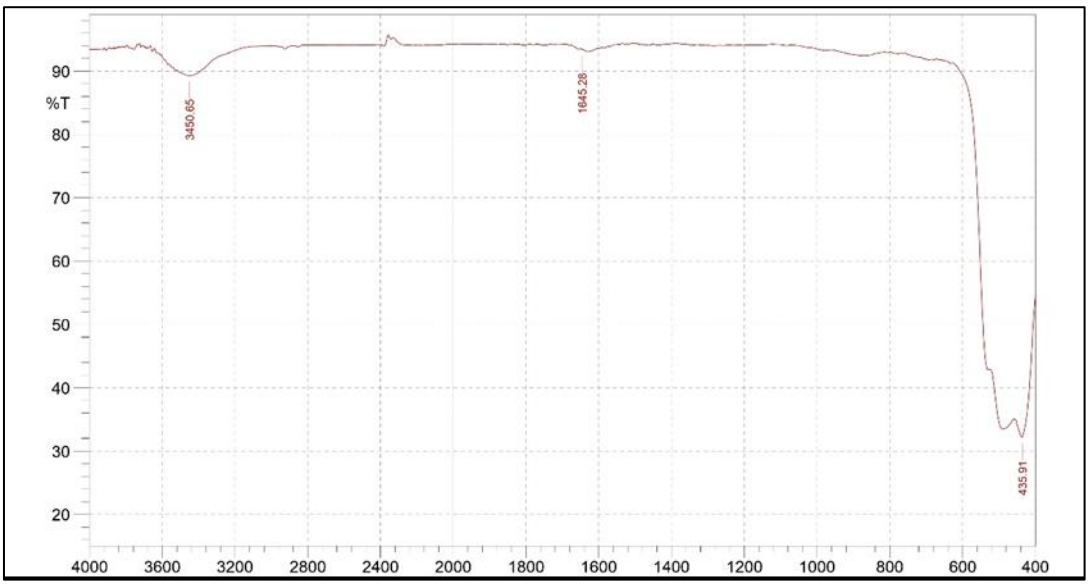

Figure 2 Zinc oxide nanoparticles (control) analyzed using Fourier Transform Infrared Spectroscopy (FTIR)

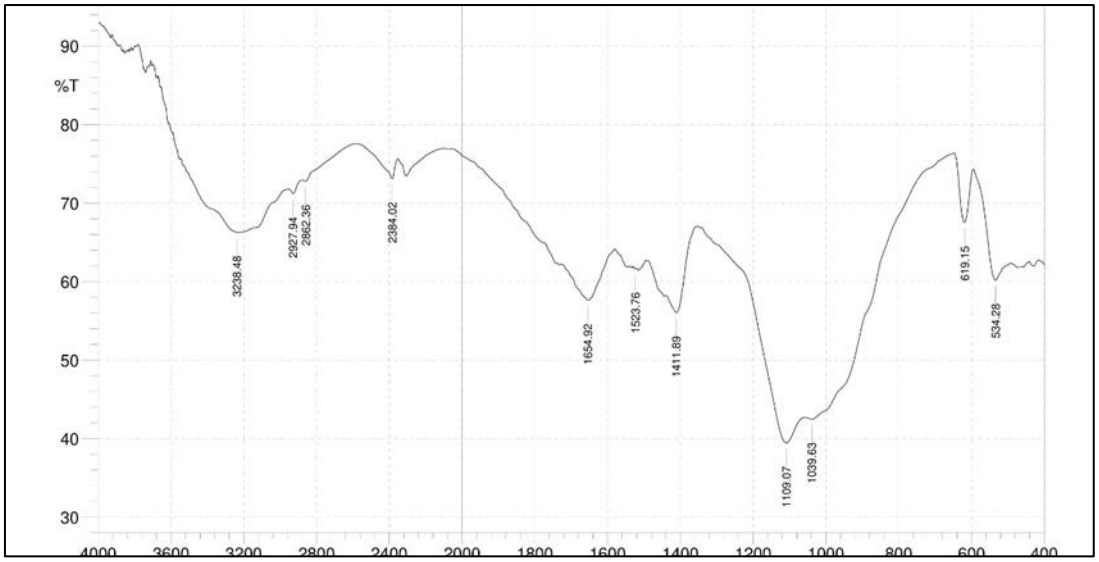

Figure 3 Biodegradation of ZnO nanoparticles by R. stolinifer at 100 mg in mineral medium with carbon source (Maltose) and nitrogen source ($NaNO_3$) at 15°C using FTIR

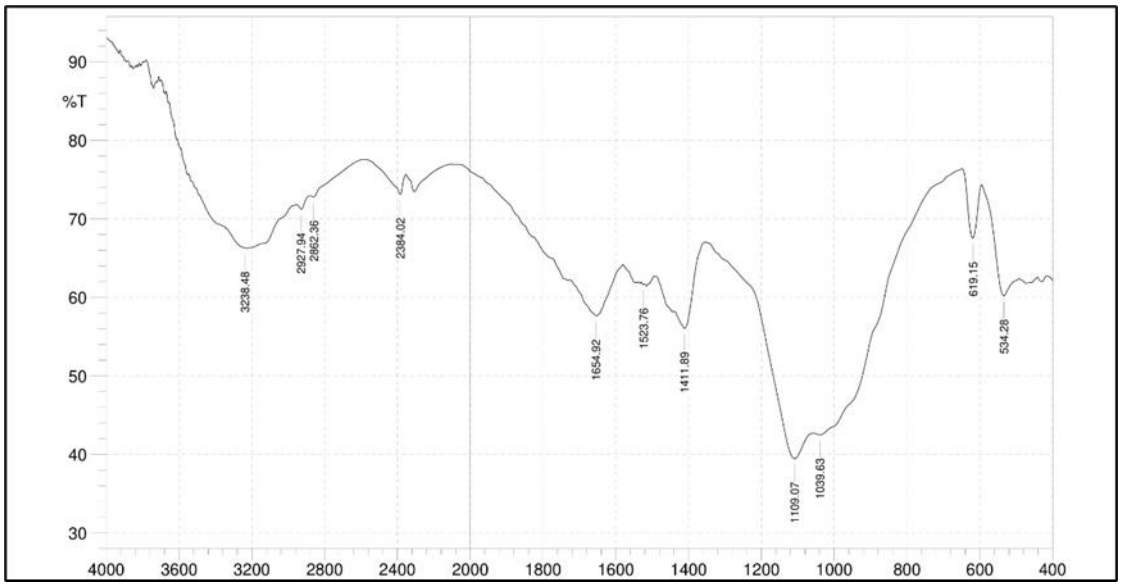

Figure 4 Biodegradation of ZnO nanoparticles by R. stolinifer at 100 mg in mineral medium with carbon source (Glucose) and nitrogen source (NH_4Cl) at 15°C using FTIR

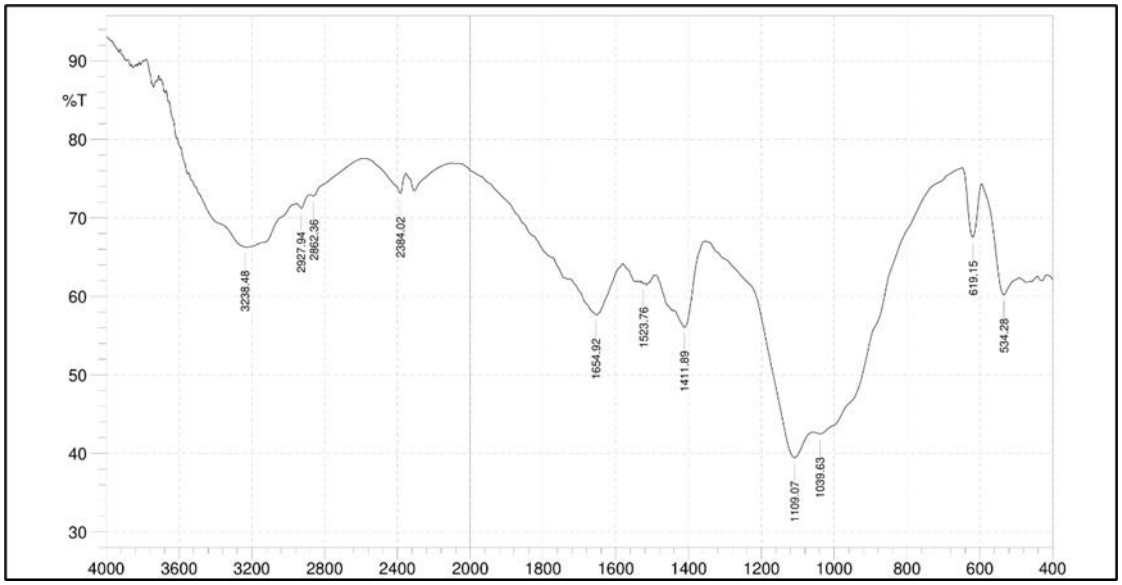

Figure 5 Biodegradation of ZnO nanoparticles by R. stolinifer at 200 mg in mineral medium with carbon source (Maltose) and nitrogen source ($NaNO_3$) at 15°C using FTIR

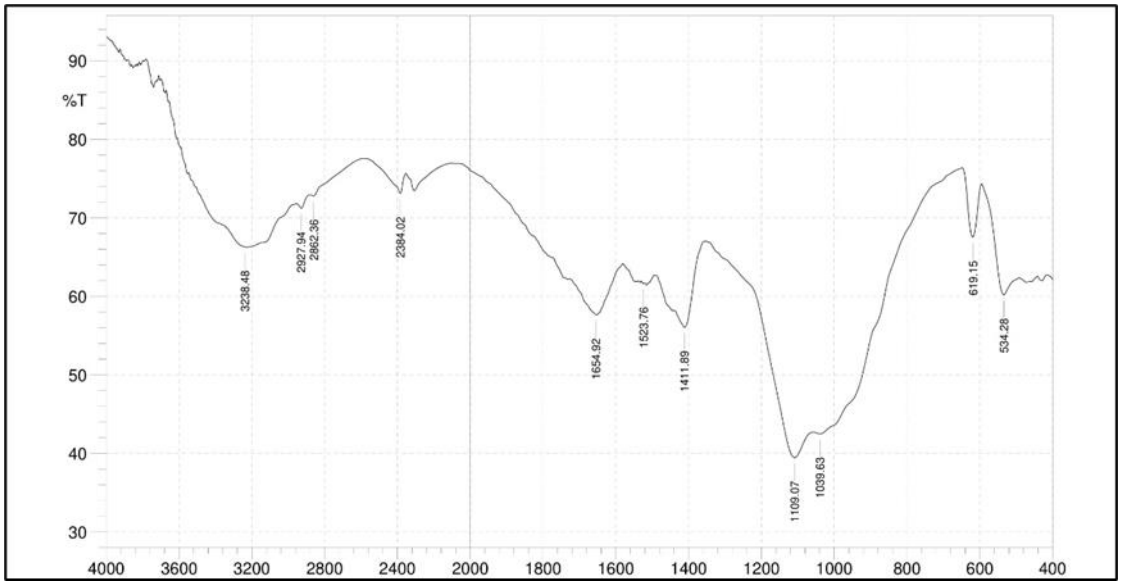

Figure 6 Biodegradation of ZnO nanoparticles by R. stolinifer at 200 mg in mineral medium with carbon source (Glucose) and nitrogen source (NH_4Cl) at 15°C using FTIR

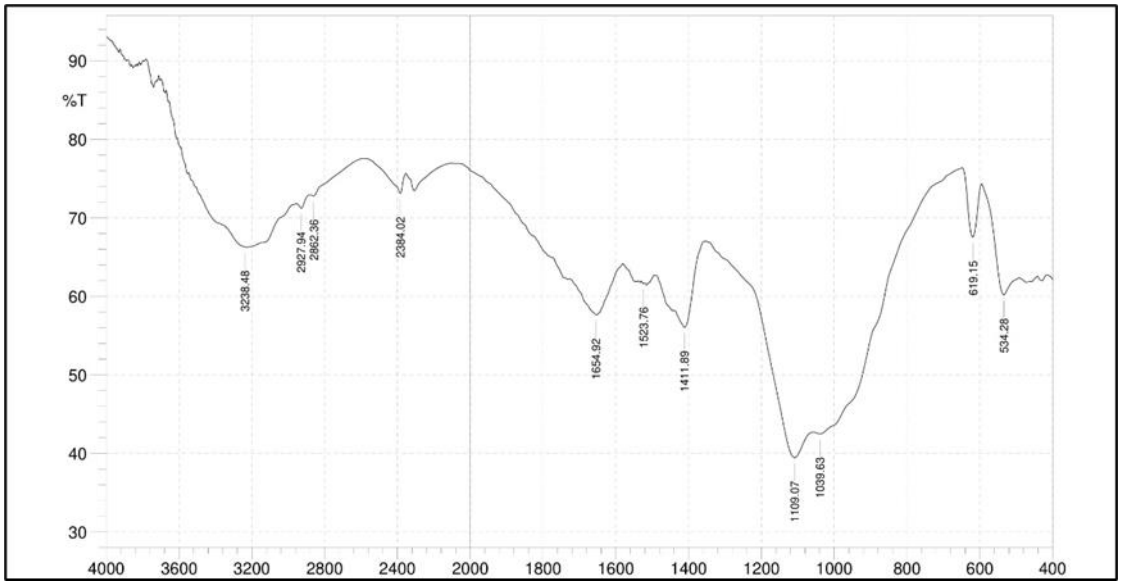

Figure 7 Biodegradation of ZnO nanoparticles by R. stolinifer at 300 mg in mineral medium with carbon source (Maltose) and nitrogen source ($NaNO_3$) at 15°C using FTIR

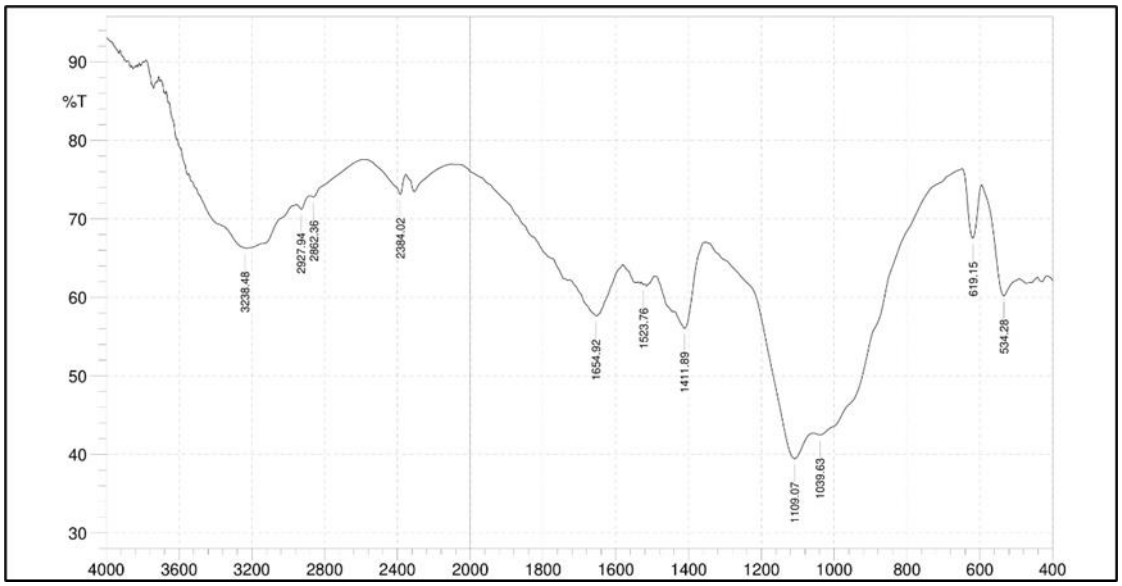

Figure 8 Biodegradation of ZnO nanoparticles by R. stolinifer at 300 mg in mineral medium with carbon source (Glucose) and nitrogen source (NH_4Cl) at 15°C using FTIR

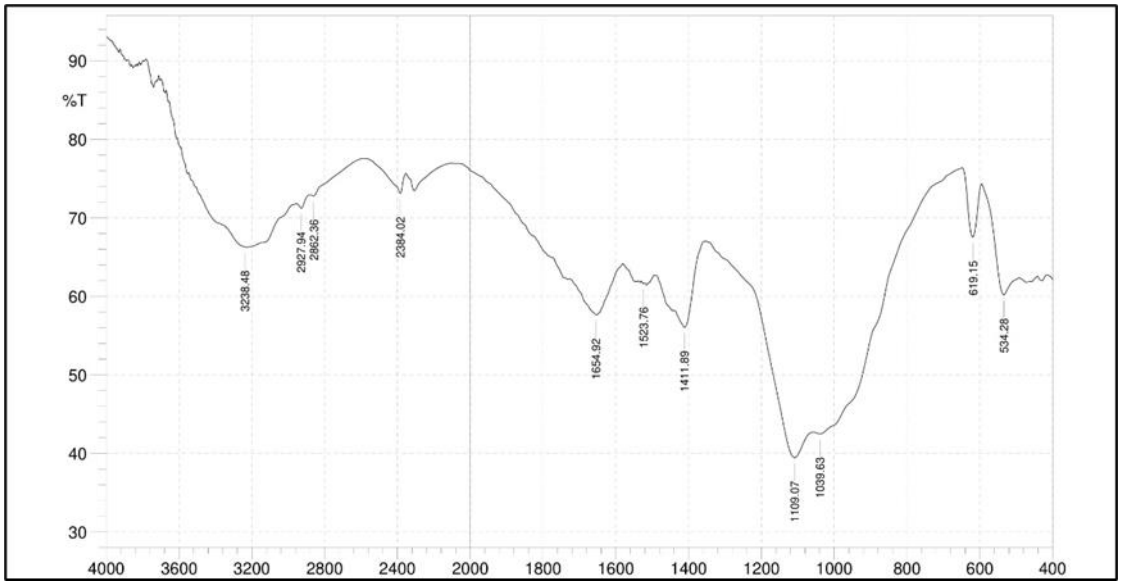

Figure 9 Biodegradation of ZnO nanoparticles by R. stolinifer at 100 mg in mineral medium with carbon source (Maltose) and nitrogen source ($NaNO_3$) at 25°C using FTIR

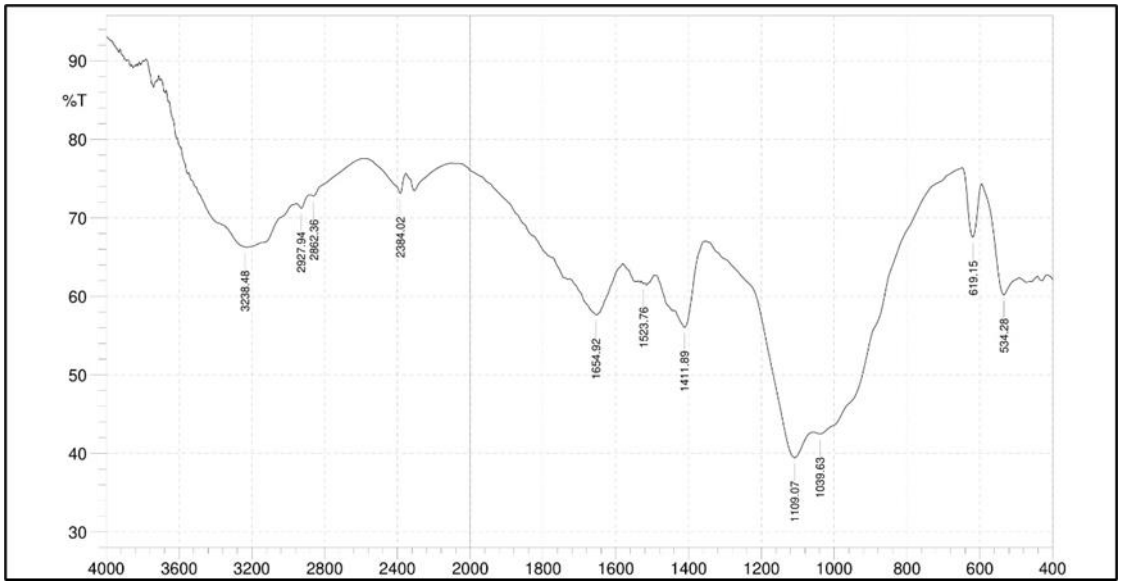

Figure 10 Biodegradation of ZnO nanoparticles by R. stolinifer at 100 mg in mineral medium with carbon source (Glucose) and nitrogen source (NH_4Cl) at 25°C using FTIR

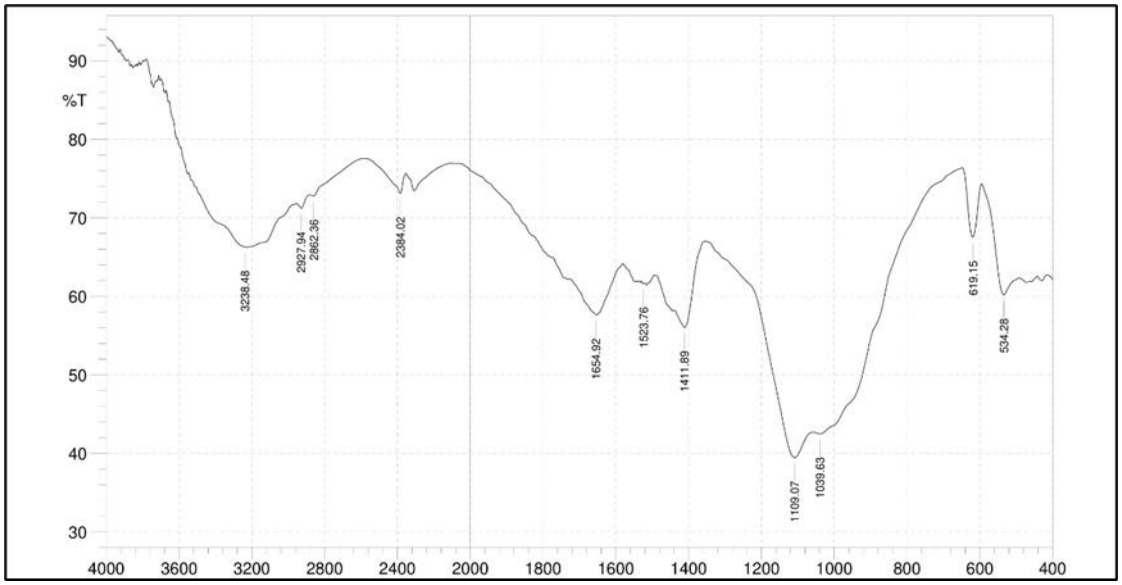

Figure 11 Biodegradation of ZnO nanoparticles by R. stolinifer at 200 mg in mineral medium with carbon source (Maltose) and nitrogen source ($NaNO_3$) at 25°C using FTIR

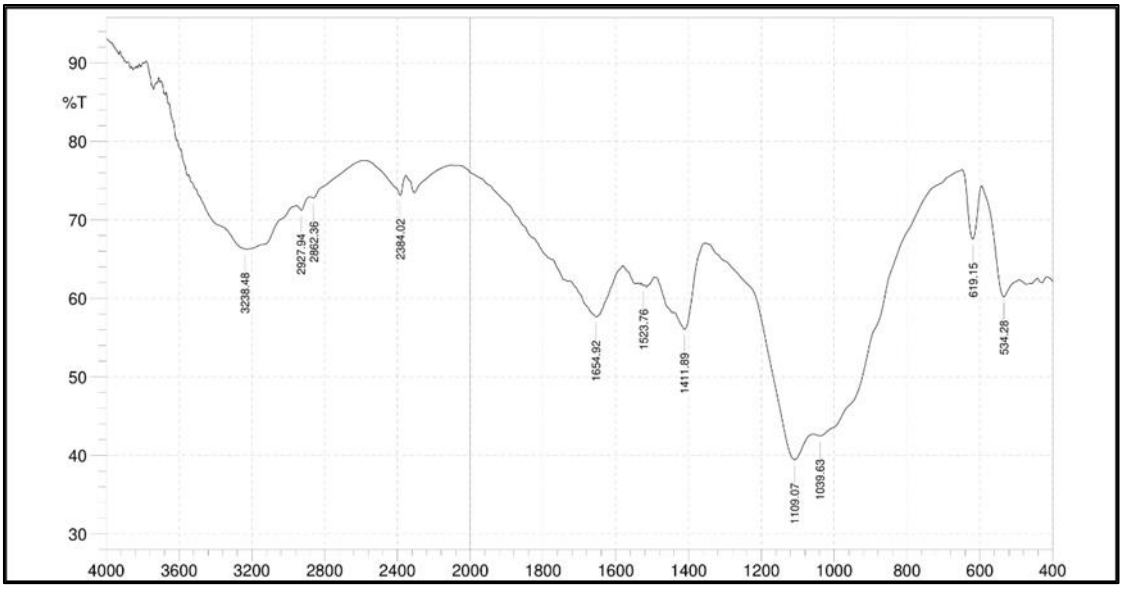

Figure 12 Biodegradation of ZnO nanoparticles by R. stolinifer at 200 mg in mineral medium with carbon source (Glucose) and nitrogen source (NH_4Cl) at 25°C using FTIR

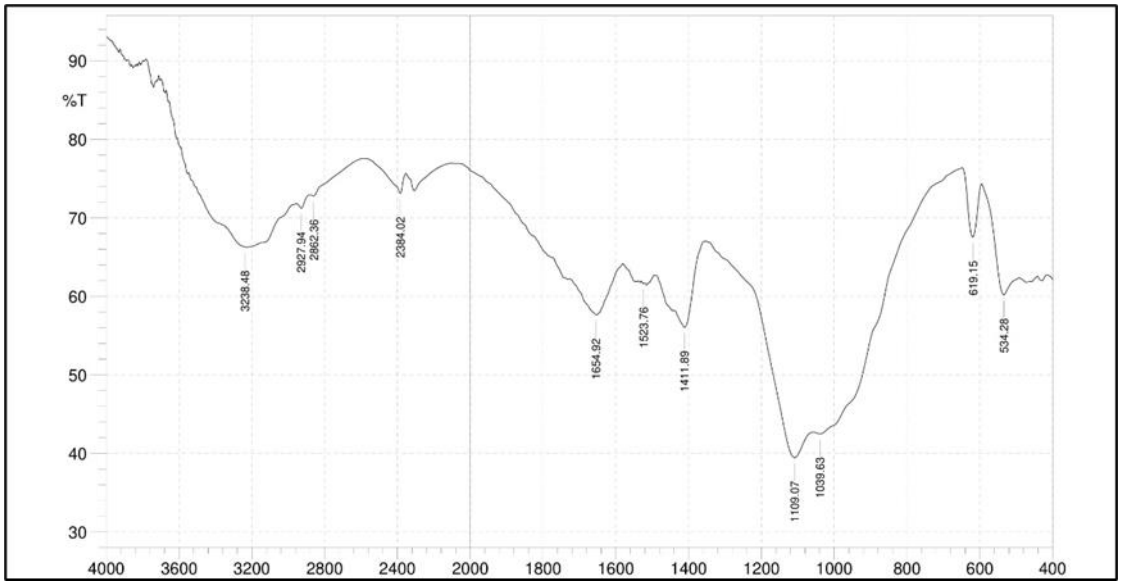

Figure 13 Biodegradation of ZnO nanoparticles by R. stolinifer at 300 mg in mineral medium with carbon source (Maltose) and nitrogen source ($NaNO_3$) at 25°C using FTIR

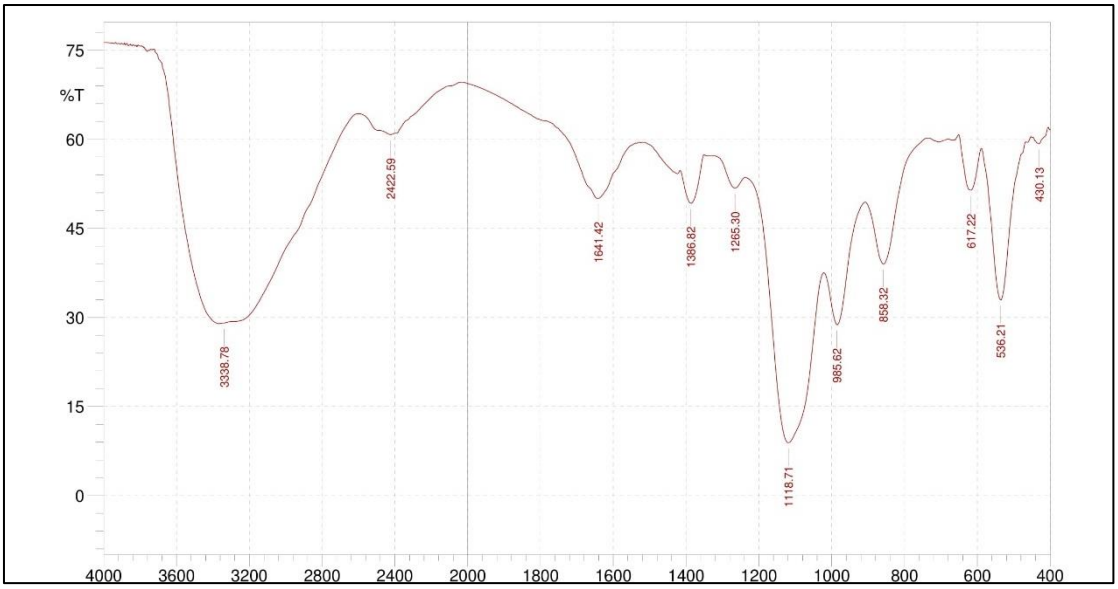

Figure 14 Biodegradation of ZnO nanoparticles by R. stolinifer at 300 mg in mineral medium with carbon source (Glucose) and nitrogen source (NH_4Cl) at 25°C using FTIR

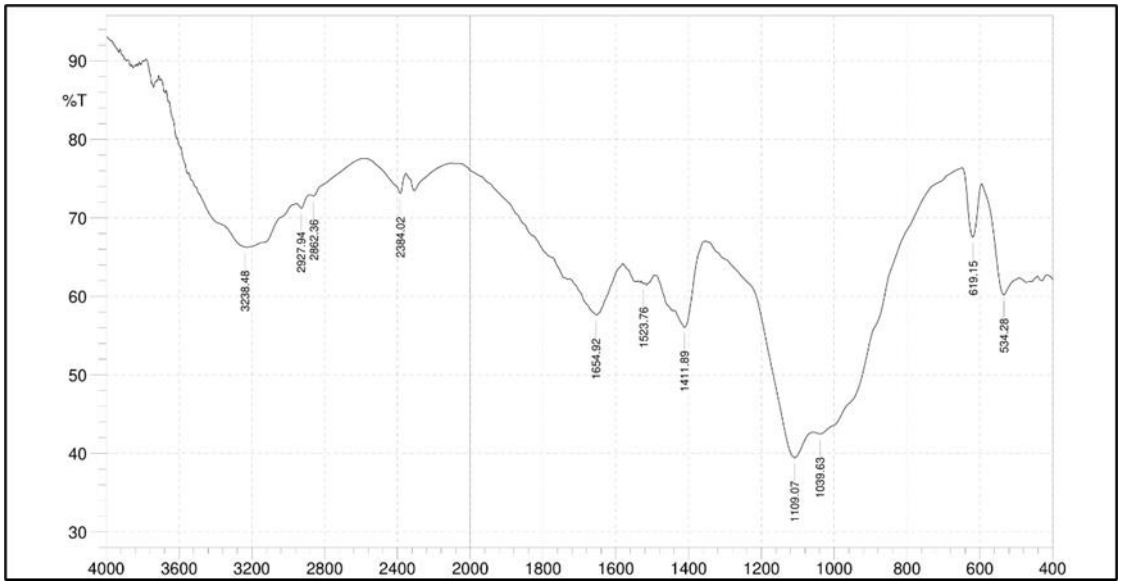

Figure 15 Biodegradation of ZnO nanoparticles by R. stolinifer at 100 mg in mineral medium with carbon source (Maltose) and nitrogen source ($NaNO_3$) at 35°C using FTIR

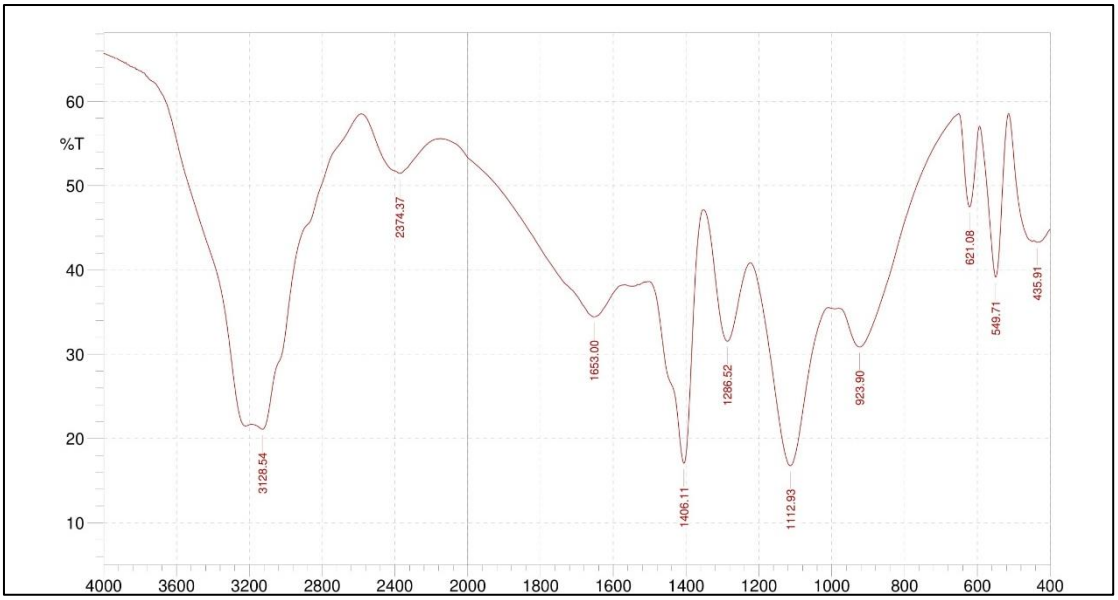

Figure 16 Biodegradation of ZnO nanoparticles by R. stolinifer at 100 mg in mineral medium with carbon source (Glucose) and nitrogen source (NH_4Cl) at 35°C using FTIR

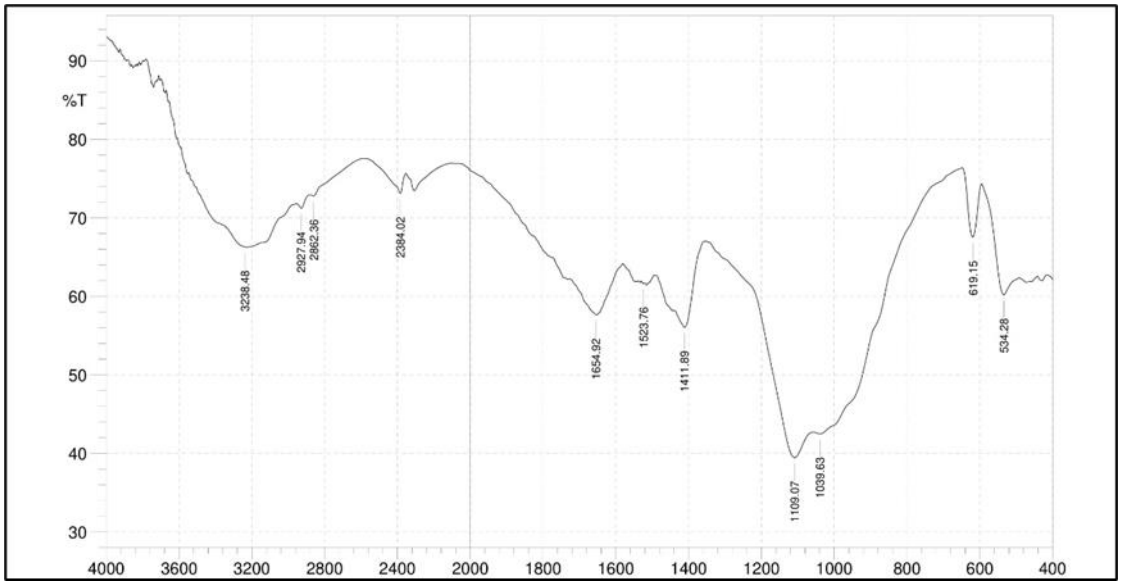

Figure 17 Biodegradation of ZnO nanoparticles by R. stolinifer at 200 mg in mineral medium with carbon source (Maltose) and nitrogen source ($NaNO_3$) at 35°C using FTIR

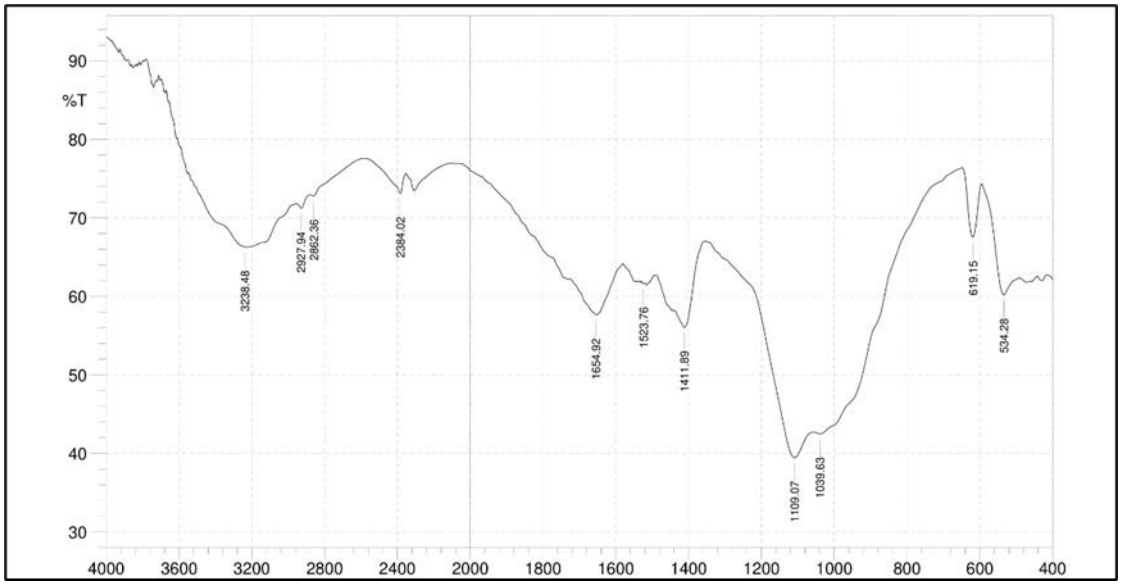

Figure 18 Biodegradation of ZnO nanoparticles by R. stolinifer at 200 mg in mineral medium with carbon source (Glucose) and nitrogen source (NH_4Cl) at 35°C using FTIR

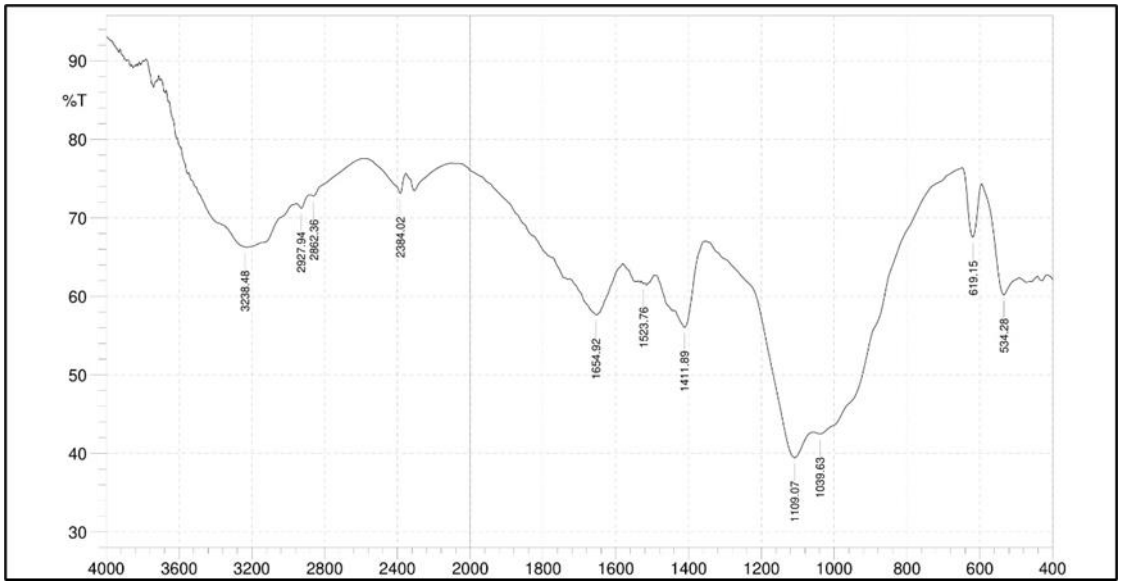

Figure 19 Biodegradation of ZnO nanoparticles by R. stolinifer at 300 mg in mineral medium with carbon source (Maltose) and nitrogen source ($NaNO_3$) at 35°C using FTIR

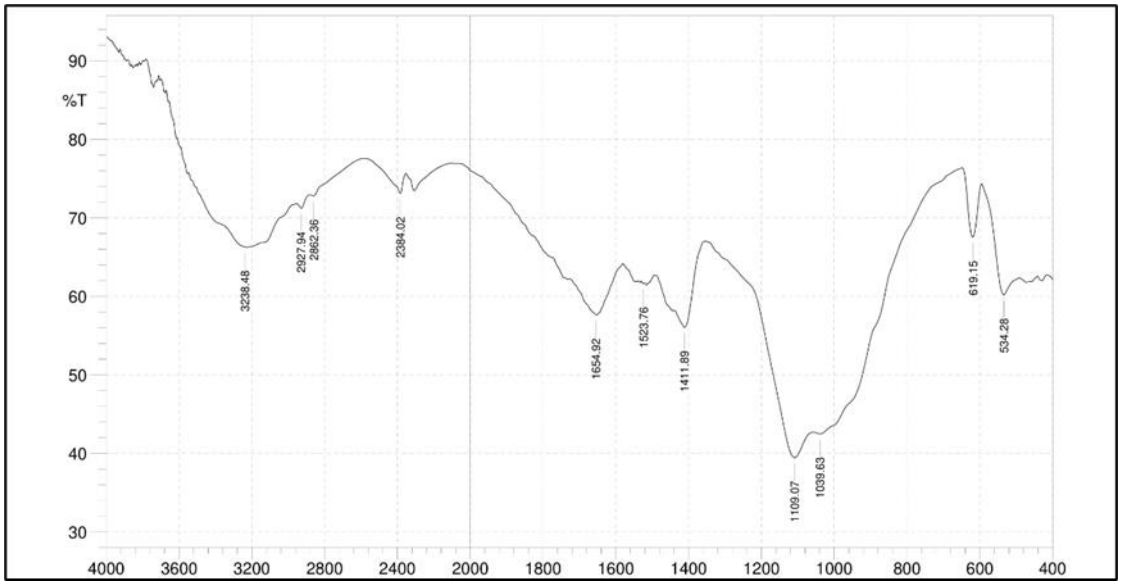

Figure 20 Biodegradation of ZnO nanoparticles by R. stolinifer at 300 mg in mineral medium with carbon source (Glucose) and nitrogen source (NH_4Cl) at 35°C using FTIR

4. Conclusion

This study confirmed that Rhizopus stolonifer isolated from agricultural soils in Abada village, Al-Fuhud district, Al-Nasiriyah, southern Iraq, has the ability to degrade zinc oxide nanoparticles (ZnO-NPs) at different concentrations (100, 200, 300 mg), using various carbon and nitrogen sources (glucose, maltose, $NaNO_3$, NH_4Cl), and under different incubation temperatures (15, 25, 35 °C). FTIR analysis showed clear changes in the spectra, such as the appearance and disappearance of bands related to ester, carboxylic acid, and hydroxyl groups, which indicate the role of the fungus in breaking down the nanoparticles.

The results also showed that changes in temperature, concentration, and nutrient sources led to differences in the rate of biodegradation, but R. stolonifer was still able to consistently transform ZnO-NPs into simpler compounds. This proves that the fungus is effective under different conditions.

Solid medium (PDA) demonstrated that colony growth of R. stolonifer remained relatively stable even with ZnO-NP exposure, confirming its adaptive capacity. This finding highlights the fungus' robust enzymatic system and its potential as a natural biodegrader across both nanoparticle and hydrocarbon pollutants.

The study therefore provides new insight into how Rhizopus stolonifer behaves in soils exposed to nanoparticles and shows its potential in reducing nanoparticle pollution. The findings highlight the role of soil fungi as natural agents that can help clean the environment and contribute to sustainable solutions for nanomaterial contamination.

Compliance with ethical standards

Disclosure of conflict of interest

No conflict of interest to be disclosed.

References

[1] Van, H. T., Hoang, V. H., Nga, L. T. Q., and Nguyen, V. Q. (2024). Effects of Zn pollution on soil: Pollution sources, impacts and solutions. Results in Surfaces and Interfaces, 17, 100360. https://doi.org/10.1016/j.rsurfi.2024.100360

[2] Xuan, L., Ju, Z., Skonieczna, M., Zhou, P. K., and Huang, R. (2023). Nanoparticles-induced potential toxicity on human health: Applications, toxicity mechanisms, and evaluation models. MedComm, 4(3), e327. https://doi.org/10.1002/mco2.327

[3] Zhou, X.-Q., Hayat, Z., Zhang, D.-D., Li, M.-Y., Hu, S., Wu, Q., Cao, Y.-F., and Yuan, Y. (2023). Zinc oxide nanoparticles: Synthesis, characterization, modification, and applications in food and agriculture. Processes, 11(4), 1193. https://doi.org/10.3390/pr11041193

[4] Šebesta, M., Urík, M., Bujdoš, M., Kolenčík, M., Vávra, I., Dobročká, E., Kim, H., and Matúš, P. (2020). Fungus Aspergillus niger processes exogenous zinc nanoparticles into a biogenic oxalate mineral. Journal of Fungi, 6(4), 210. https://doi.org/10.3390/jof6040210

[5] Elkady, F. M., Badr, B. M., Saied, E., Hashem, A. H., Abdulrahman, M. S., Alkherkhisy, M. M., Selim, T. A., Alshabrmi, F. M., Alatawi, E. A., Aba Alkhayl, F. F., Salama, A., Mansy, M. S., and Aufy, M. (2025). Mycosynthesis of zinc oxide nanoparticles using Mucor racemosus with their antimicrobial, antibiofilm, anticancer and antioxidant activities. Scientific Reports, 15, 18772. https://doi.org/10.1038/s41598-025-03421-w

[6] Cappuccino, J. G., and Sherman, N. (1987). Microbiology: A laboratory manual. Benjamin Cummings Publishing Co. Inc. (California, Amsterdam, Sydney). p 120.

[7] Kapilan, R. (2015). Enzyme Production by Rhizophus stolonifer Isolated from Bread and Kinetic Properties of the Extracellular Amylase. Jacobs Journal of Enzymology and Enzyme Engineering, 1(1), 005. https://www.researchgate.net/publication/291357539

[8] Liu, Q., Chen, Q., Liu, H., Du, Y., Jiao, W., Sun, F., and Fu, M. (2024). Rhizopus stolonifer and related control strategies in postharvest fruit: A review. Heliyon, 10(4), e29522. https://doi.org/10.1016/j.heliyon.2024.e29522

[9] Nafady, N. A., Alamri, S. A. M., Hassan, E. A., Hashem, M., Mostafa, Y. S., and Abo-Elyousr, K. A. M. (2019). Application of ZnO-nanoparticles to manage Rhizopus soft rot of sweet potato and prolong shelf-life. Folia Horticulturae, 31(2), 319–329. https://doi.org/10.2478/fhort-2019-0025

[10] Liu, Q., Chen, Q., Liu, H., Du, Y., Jiao, W., Sun, F., and Fu, M. (2024). Rhizopus stolonifer and related control strategies in postharvest fruit: A review. Heliyon, 10(2), e29522. https://doi.org/10.1016/j.heliyon.2024.e29522

[11] Ibrahim, M., and Shehu, K. (2015). Effects of various carbohydrates on the growth of Rhizopus stolonifer. International Journal of Multidisciplinary Research and Development, 2(5), 306–308.

[12] Fothergill, P. G., and Yeoman, M. M. (1957). The mineral nutrition of Rhizopus stolonifer. Journal of General Microbiology, 17(3), 631–689. https://doi.org/10.1099/00221287-17-3-631

[13] Amiri, A., Chai, W., and Schnabel, G. (2011). Effect of nutrient status, pH, temperature and water potential on germination and growth of Rhizopus stolonifer and Gilbertella persicaria. Journal of Plant Pathology, 93(3), 603–612. Retrieved from https://www.researchgate.net/publication/288226830

[14] Zaveri, A., Edwards, J., and Rochfort, S. (2022). Production of primary metabolites by Rhizopus stolonifer, causal agent of almond hull rot disease. Molecules, 27(21), 7199. https://doi.org/10.3390/molecules27217199

[15] Chakra, P. S., Banakar, A., Puranik, S. N., Kaveeshwar, V., Ravikumar, C. R., and Gayathri, D. (2025). Characterization of ZnO nanoparticles synthesized using probiotic Lactiplantibacillus plantarum GP258. Beilstein Journal of Nanotechnology, 16(1), 78–89. https://doi.org/10.3762/bjnano.16.8

[16] Al-Jawhari, I. F. (2014). Biodegradation of kerosene by Aspergillus niger and Rhizopus stolonifer. Journal of Applied and Environmental Microbiology, 2(1), 31–36. Retrieved from https://www.researchgate.net/publication/275770512

[17] Sumanth, B., Lakshmeesha, T. R., Ansari, M. A., Alzohairy, M. A., Udayashankar, A. C., Shobha, B., Niranjana, S. R., Srinivas, C., and Almatroudi, A. (2020). Mycogenic synthesis of extracellular zinc oxide nanoparticles from Xylaria acuta and its nanoantibiotic potential. International Journal of Nanomedicine, 15, 8519–8536. https://doi.org/10.2147/IJN.S271743

[18] Al-Jawhari, I. F. (2016). Ability of sediments fungi in biodegradation of diesel fuel. International Journal of Pure and Applied Bioscience, 4(2), 27–37. Retrieved from https://www.researchgate.net/publication/304658566

[19] Mishra, D. N., Prasad, L., and Suyal, U. (2025). Synthesis of zinc oxide nanoparticles using Trichoderma harzianum and its bio-efficacy on Alternaria brassicae. Frontiers in Microbiology, 16, 1506695. https://doi.org/10.3389/fmicb.2025.1506695